Supplementary Information

Supplementary Methods

Data pre-processing, covariate correction, and differential expression

Several technical and sample covariates can bias gene expression values inferred from our microarray data, such as array batch effects and individual ethnicity, gender. These covariates can greatly confound downstream analyses, resulting in false positive and negative associations and reducing the power of statistical analyses. We corrected for these biases in three ways: by normalizing to "reference" probes (control probes with a fixed fluorescence value that control for the geometry and preparation of the array), by applying batch normalization using ComBat [1], and by correcting for observed covariates (gender, age, and collection site) using robust linear regression. The residuals after these corrections were then used as the gene expression values for downstream analyses. Differential expression analysis was performed using the Significance Analysis of Microarrays (SAM) [2]. Genes shown in Figure S1B had the highest gene expression difference and were deemed significantly up or down regulated with a false discovery rate of 5%.

Graph convolution for eQTL discovery

Integrating gene-gene relationships has been shown to increase the power of cis-eQTL discovery [3]. Here, we leveraged our co-expression networks for the heart failure and control groups for eQTL discovery by performing graph convolution with an identity kernel to the gene expression matrix for each group prior to eQTL regressions. Specifically, we applied the following transformation for each group separately:

$$CE = (I - D^{-½} AD^{-½})E$$

Where E is the expression matrix of the cohort, A is the adjacency matrix of the network, D is the degree matrix of A, and I is the identity matrix. The resulting CE is then used downstream for eQTL discovery.

Global and local topological parameters for gene ranking

After inferring the gene co-expression networks and gene communities for both cohorts, we calculated topological properties for each gene in each network in order to get a sense of a gene's role in the networks and in the context of known pathways and gene sets. To this end, we defined a gene's *g* global connectivity (*GC*) as the number of gene groups (e.g. pathways) in a set that were differentially connected in *g*'s neighborhood. We achieved this by the following procedure (see Figure S6):

1. We first ranked the neighbors of *g* by their absolute connection weight (e.g. correlation) to *g* in both the HF and control networks. This resulted into two ranked list.

2. For each pathway/gene set, we calculated the enrichment in the difference of rankings using the Kolmogorov-Smirnov (KS) statistic (analogous to gene set enrichment analysis [4])
3. We assessed significance of each statistic using the standard KS test with a Benjamini-Hochberg correction with a false discovery rate of 5%.

To capture local perturbations without any pathway/gene set context, we defined the local connectivity metric *LC* for a gene *g* used for this purpose was calculated as follows:

$$LC(g) = deg\_norm(g, HF\_net) - deg\_norm(g, Control\_net)$$

Where *deg_norm(g, net)* is the max-normalized degree of gene *g* in network *net* (divided by the maximum degree across all genes).

Isolation, culture, perturbation, and visualization of NRVMs

NRVMs were isolated using standard collagenase protocols as described previously and cultured in serum-free DMEM media. In order to attenuate the effects of fibroblast contamination and accentuate metabolic changes, no glucose was added to the media and a final concentration of 20 μM of the fibroblast inhibitor Ara-C (Sigma-Aldritch) was incorporated. Furthermore, for robust expression measurements at least 1 million cells were plated in a 12-well plate, corresponding to at least 70% confluency. For phenylephrine-treated cells, 50-μM of phenylephrine was added 48 hours after isolation. For the knockdown experiments, cells were transfected either with a siRNA targeted to PPP1R3A (Stealth siRNA, Invitrogen) or a scrambled siRNA using the RNAiMAX system (Invitrogen) according to manufacturer instructions; transfections were performed 24 hours after isolation. RNA extraction was performed using the Qiagen RNeasy kit according to manufacturer instructions and were DNAse-treated using the DNA-free RNA kit from Zymo research. CDNA was synthesized with the High-capacity cDNA reverse transcription kit from ABI and qRT-PCR assays were performed using KAPA SYBR FAST on a ViiA 7 ABI system.

For visualization, cells were fixed directly in the culture plate wells using 4% PFA in room temperature for 10 minutes, permeabilized with 0.2% Triton-X in room temperature for 10 minutes, and blocked with DAKO protein block in room temperature for 30 minutes. Afterwards, fixed cells were incubated in mouse anti-sarcomeric α-actinin antibody (Sigma) in DAKO antibody buffer overnight at 4 C. Alexa secondary antibodies were added the next day after PBS washes and the cells were incubated for one hour at room temperature. Cells were then washed with PBS and the nuclei were stained with DAPI (AntiFade DAPI, Invitrogen). Fluorescent cells were then imaged at 40X or 20X magnification using an Olympus BX-51 inverted fluorescent microscope. Cell area was quantified with ImageJ.

Supplementary References

1. Leek, J. T., Johnson, W. E., Parker, H. S., Jaffe, A. E. & Storey, J. D. The sva package for

removing batch effects and other unwanted variation in high-throughput experiments. *Bioinformatics* **28,** 882–883 (2012).

2. Tusher, V. G. G., Tibshirani, R. & Chu, G. Significance analysis of microarrays applied to the ionizing radiation response. *Proceedings of the National Academy of Sciences* **98,** 5116–5121 (2001).
3. Mizrachi, E. *et al.* Network-based integration of systems genetics data reveals pathways associated with lignocellulosic biomass accumulation and processing. *Proc. Natl. Acad. Sci. U. S. A.* **114,** 1195–1200 (2017).
4. Subramanian, A. *et al.* Gene set enrichment analysis: a knowledge-based approach for interpreting genome-wide expression profiles. *Proc. Natl. Acad. Sci. U. S. A.* **102,** 15545–15550 (2005).

Supplementary Figures

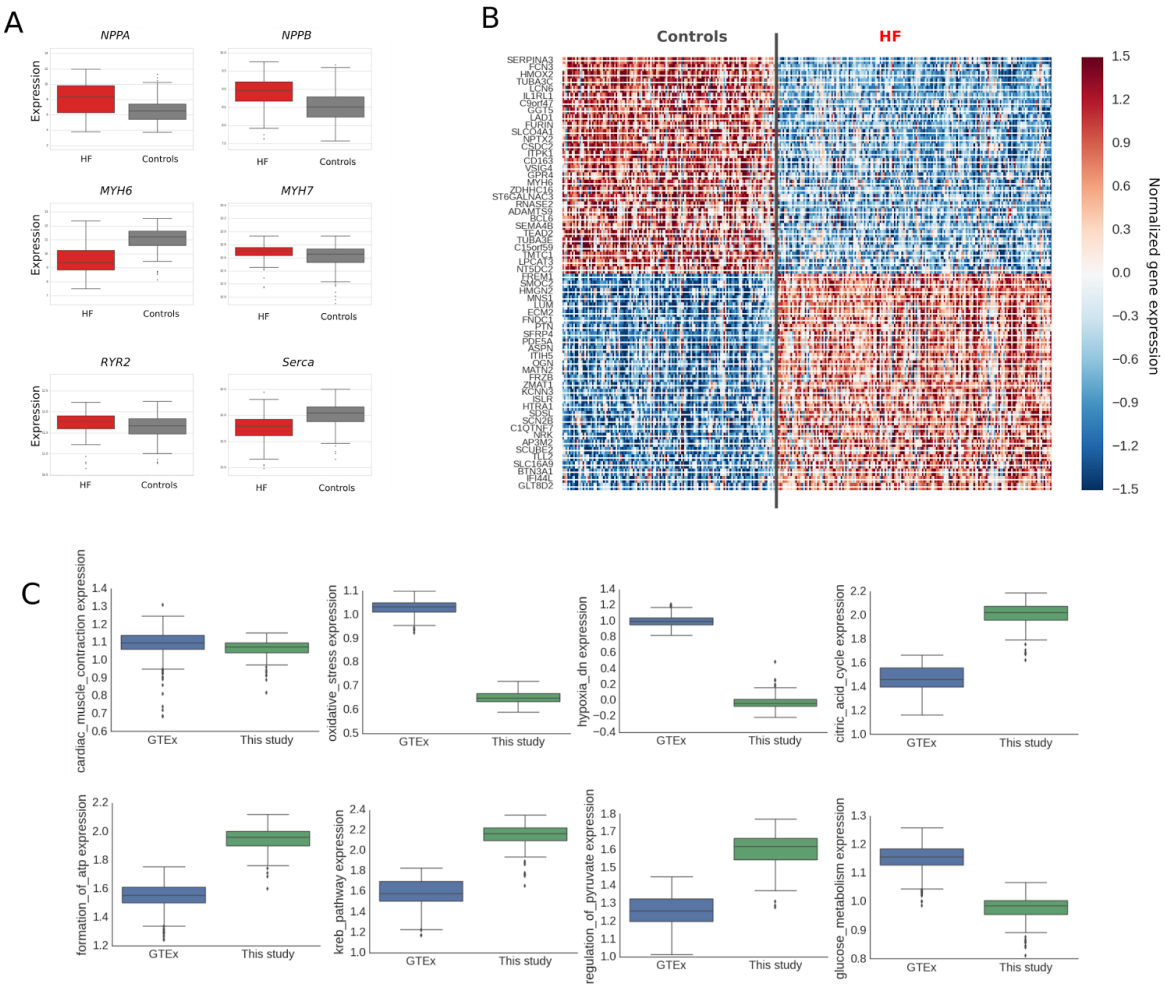

Figure S1: (A) Expression of various genes involved in heart failure in the failing and non-failing control cohorts. (B) Top differentially expressed genes between failing and non-failing controls. (B) Mean expression of various gene sets, including metabolic pathways and oxidative stress/hypoxia genes of the GTEx post-mortem samples (blue) and the control cohort in this study (green) obtain from heart transplant donor hearts.

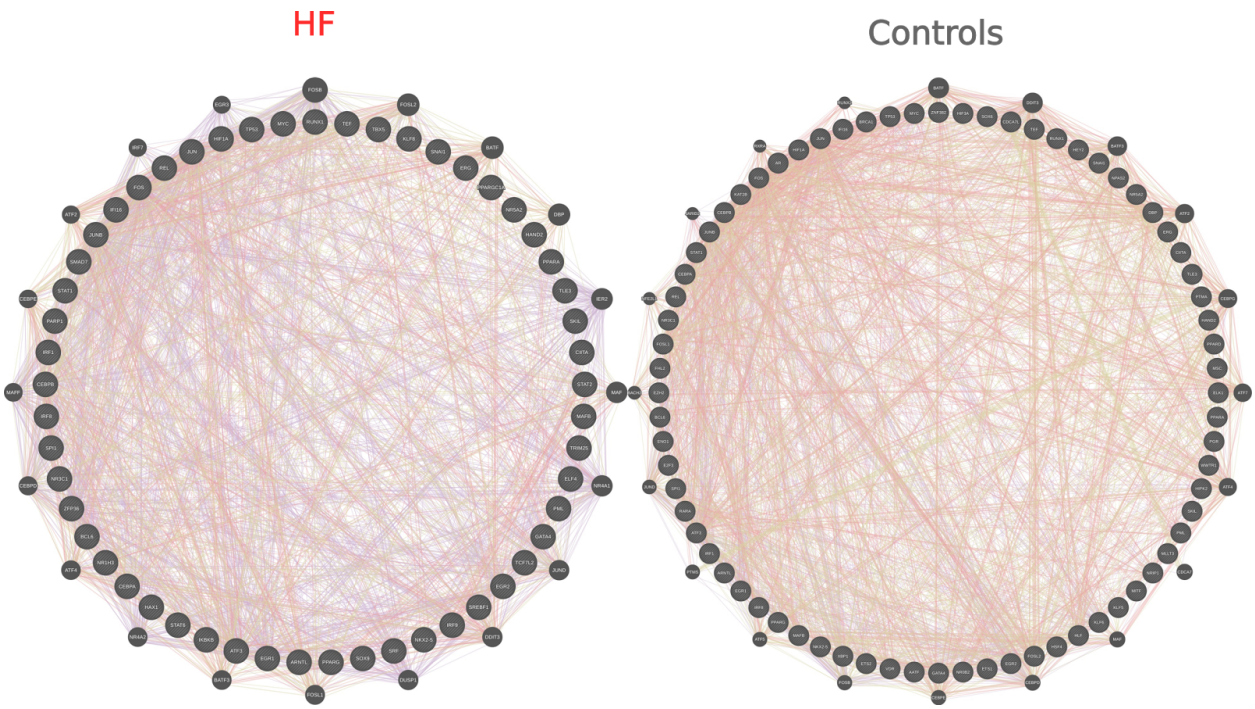

Figure S2: Co-expression (purple), physical interaction (red), and shared domain (green) relationships between top connected transcription factors in the heart failure and non-failing control networks. Both sets of genes are densly connected, suggesting coordination between the top regulators of both networks.

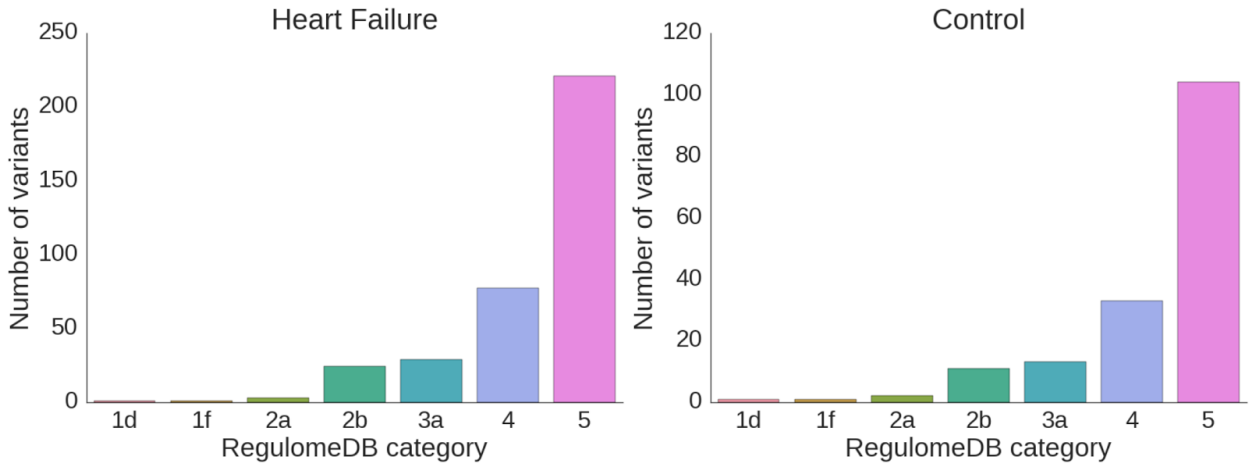

Figure S3: Number of eQTLs for each network for which there were RegulomeDB annotations. RegulomeDB categories are defined as follows: category 1 are known eQTLs with ENCODE DNase sensitivity peaks (1f) and TF binding data (1d); category 2 only have evidence of TF binding (2b) and DNase sensitivity peaks as well as a matching TF binding motif (2a); category 3a have predicted TF binding and a TF motif as well as DNase peak; category 4 have predicted TF binding and a DNase peak; and category 5 have either predicted TF binding or a DNase

peak.

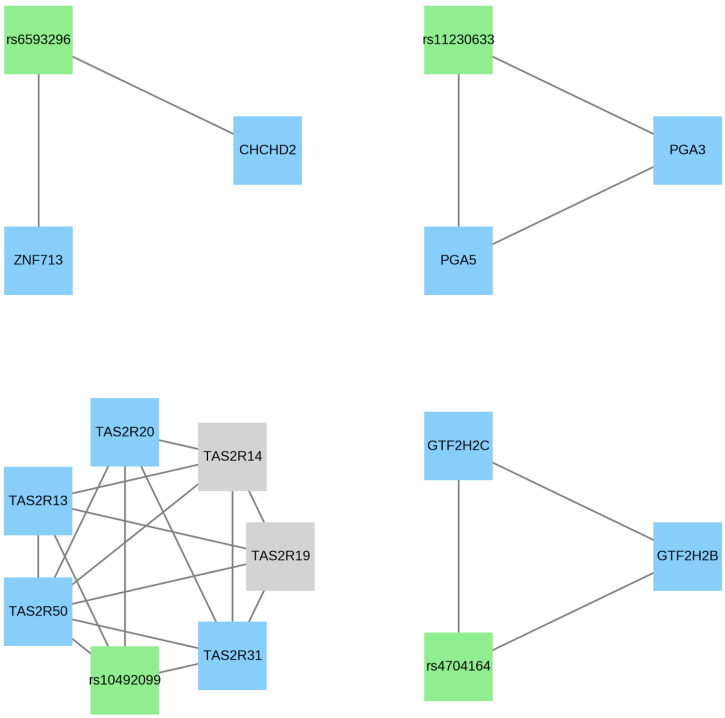

Figure S4: Connected components of the QTL-gene-interaction network for the non-failing control cohort. eQTL variants are drawn in green, genes associated with the variant are drawn in blue, and other genes connected to the associated genes via the co-expression network are drawn in gray.

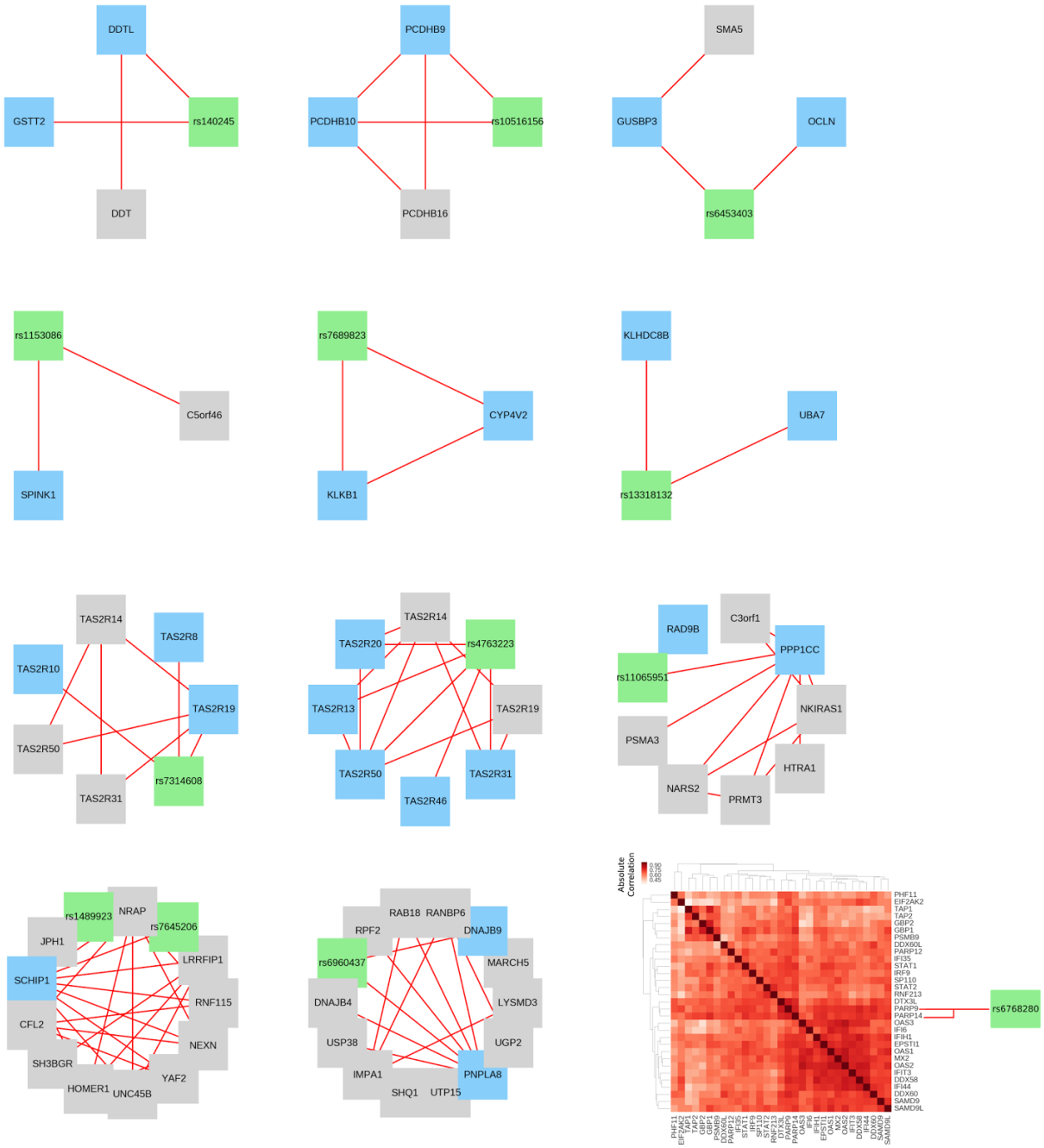

Figure S5: Connected components of the QTL-gene-interaction network for the heart failure control cohort. eQTL variants are drawn in green, genes associated with the variant are drawn in blue, and other genes connected to the associated genes via the co-expression network are drawn in gray.

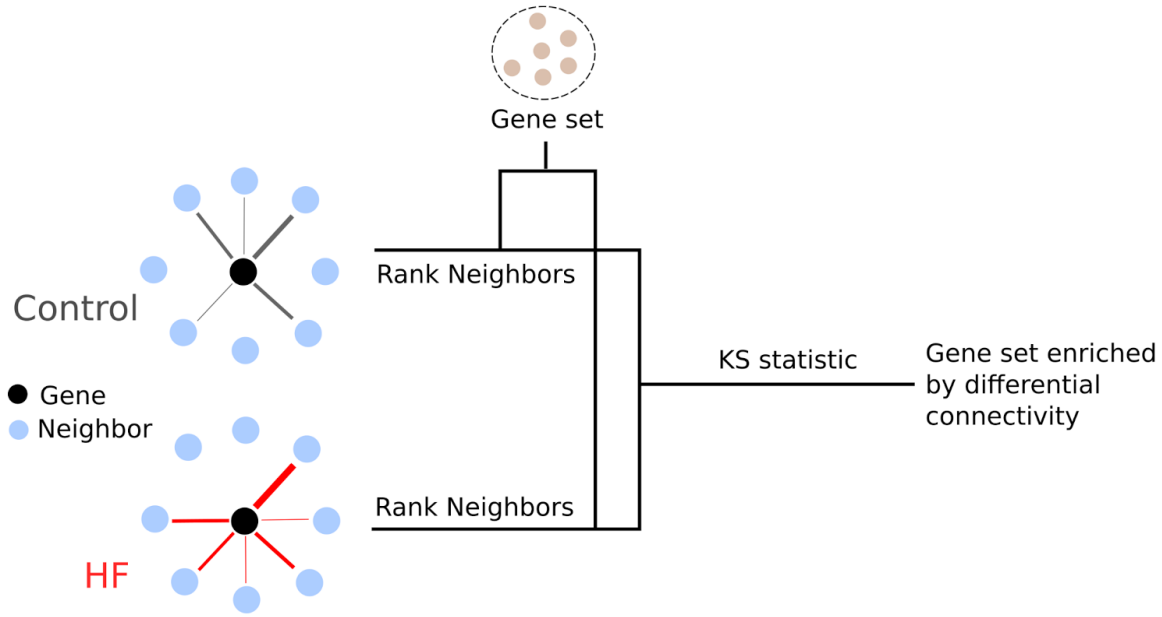

Figure S6: Calculation of the differential global connectivity (GC) of a gene with known gene sets. We take the gene's neighborhood in the heart failure and control network and rank the neighbors by their connectivity strength. We then calculate enrichment of a gene set (e.g. HCM pathway genes) in each ranked list and calculate the difference via a Kolmogorov-Smirnov test.

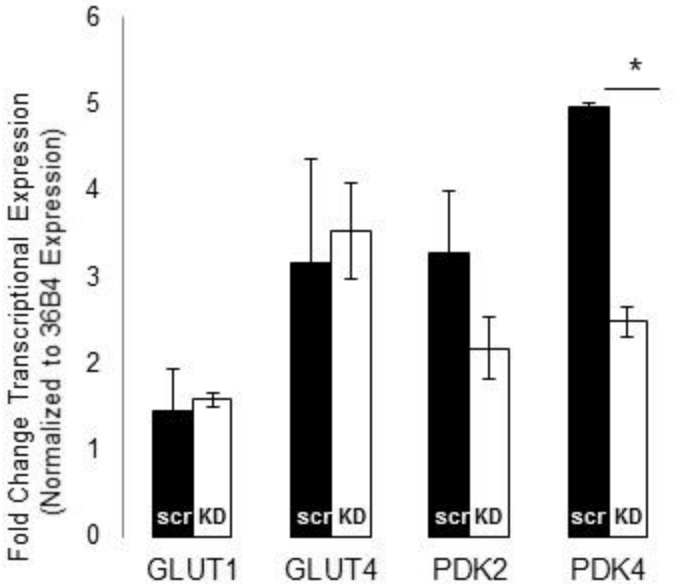

Figure S7: Differences in expression levels of key metabolic genes between *PPP1R3A* knockdowns (white) and scrambled controls (black) as confirmed via qPCR.

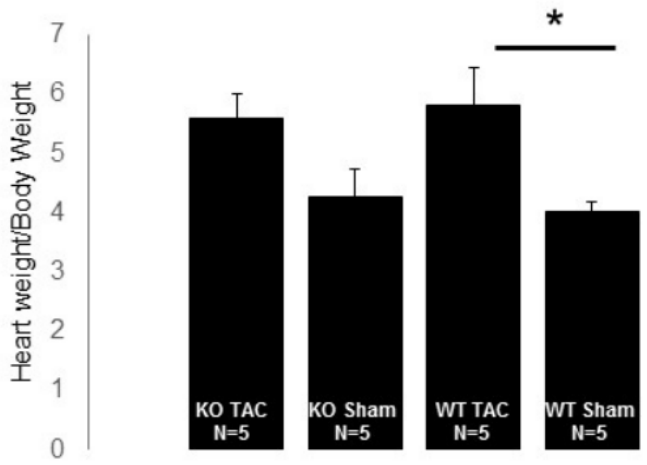

Figure S8: Heart weight differences between wild type and *PPP1R3A* knockout mice after TAC surgery/treatment and a sham control.